9243

244

Copy
RM L54B16

NACA RM L54B16

TECH LIBRARY KAFB, NM
0144274

7525

NACA

RESEARCH MEMORANDUM

COMPARISON OF EXPERIMENTAL WITH CALCULATED RESULTS FOR THE LIFTING EFFECTIVENESS OF A FLEXIBLE 45° SWEPTBACK WING OF ASPECT RATIO 6.0 AT MACH NUMBERS FROM 0.8 TO 1.3

By Richard E. Walters

Langley Aeronautical Laboratory
Langley Field, Va.

NATIONAL ADVISORY COMMITTEE
FOR AERONAUTICS

WASHINGTON
April 15, 1954

CONFIDENTIAL

TECH LIBRARY KAFB, NM
0144274

1N

NATIONAL ADVISORY COMMITTEE FOR AERONAUTICS

RESEARCH MEMORANDUM

COMPARISON OF EXPERIMENTAL WITH CALCULATED RESULTS FOR THE LIFTING EFFECTIVENESS OF A FLEXIBLE 45° SWEPTBACK WING OF ASPECT RATIO 6.0 AT MACH NUMBERS FROM 0.8 TO 1.3

By Richard E. Walters

SUMMARY

Tests were conducted on models having 45° sweptback wings with varying degrees of flexibility to determine the effective lift-curve slopes in order to evaluate the usefulness of a general method for the prediction of the effective lift ratio by a comparison of the predicted values with the test results. Tests were made with three aspect-ratio-6.0 taper-ratio-0.6 wings having 45° sweepback of the quarter-chord line and NACA 65A009 streamwise airfoil sections. The Mach number range covered was from 0.8 to 1.3.

Curves of the lift-curve slope and pitch damping are presented. The effective lift ratio $C_{L_{\alpha_e}}/C_{L_{\alpha_r}}$ as determined from the experimental results and from a representative method of prediction is shown as a function of the load flexibility parameter $C_{L_{\alpha_r}} qk$ for purposes of comparison. A comparison is also made of the effect of different assumed load distributions and of different assumed centers of pressure on the predicted effective lift ratio.

The results of the tests showed that these methods predicted values of the effective lift-slope ratio which were within 5 percent of the experimental values.

INTRODUCTION

With the increased use of thin, sweptback wings of high aspect ratio, the problem of elastic deformation has assumed primary significance. The

aerodynamic characteristics of the wing can no longer be considered independently of the structural deflections since the effect of wing bending and torsion on the sectional angle of attack has become appreciable.

There have been many and varied attempts to predict and evaluate the change in the lifting effectiveness of a sweptback wing as the wing is allowed to deflect under load (for example, refs. 1 to 3). The method of reference 1 is the most general in nature and allows the application of both arbitrary load distributions and wing construction to the problem. In most approaches, however, it has been necessary to compromise either the structural or aerodynamic aspects in order to obtain a solution. (See refs. 2 and 3.) The purpose of this paper is to compare the general methods suggested for the solution with the experimental results of flight tests of a representative sweptback wing of varying degrees of flexibility.

In the following analysis the deformation of the structure is expressed in terms of a set of experimentally determined structural influence coefficients. Different types of load distributions are assumed and applied to the influence coefficients in order to determine the predicted effective lift. There are three comparisons to be made: first, that between the predicted values of the effective lift and the experimental results; second, that between values predicted by assuming different load distributions in the calculations; and thirdly, that between values predicted by assuming different center-of-pressure positions.

The experimental results were determined from flight tests of three rocket-powered models with the same wing plan forms but varying degrees of wing flexibility. The wings were of aspect ratio 6.0 and taper ratio 0.6, and had NACA 65A009 free-stream airfoil sections. The variation in wing flexibility was due to the differences in the wing inlays which were 0.064-inch Inconel, 0.032-inch Inconel, and 0.064-inch 24S-T aluminum alloy.

The Mach number range covered was approximately 0.8 to 1.3 and the Reynolds number range was 3.0×10^6 to 8.0×10^6 based on wing mean aerodynamic chord. The models were flown at the Langley Pilotless Aircraft Research Station at Wallops Island, Va.

SYMBOLS

a_n	normal acceleration, g units
b	wing span, ft
c	chord, ft

$\bar{c}$	mean aerodynamic chord
C_L	lift coefficient, $\frac{L}{qS}$
C_{L_α}	lift-curve slope, 57.3 $\frac{dC_L}{d\alpha}$, per radian
$C_{L_{\alpha_e}}$	effective lift-curve slope of flexible wing
$C_{L_{\alpha_r}}$	rigid-wing lift-curve slope
c_{l_α}	section lift-curve slope
C_m	pitching-moment coefficient, $\frac{M}{qS\bar{c}}$
$C_{m_q} + C_{m_{\dot{\alpha}}}$	damping-in-pitch coefficient, $\frac{\partial C_m}{\partial \frac{\dot{\theta}c}{2V}} + \frac{\partial C_m}{\partial \frac{\dot{\alpha}c}{2V}}$, per radian
g	acceleration due to gravity, 32.2 ft/sec^2
k	stiffness parameter, $\frac{\theta/L}{(\theta/L)_{ref}}$
L	lift, lb
M	pitching moment, ft-lb
N	normal force, lb
P	load, lb
q	dynamic pressure, lb/sq ft
r	body radial coordinate, in.
Δs	area of reference panel, sq ft
S	wing area, sq ft

[redacted]

T	torque, in-lb
w	weight of reference panel, lb
W	total configuration weight, lb
x	longitudinal body coordinate, in.
y	spanwise coordinate normal to fuselage center line
α	angle of attack, deg
$\bar{\alpha}$	local angle of attack of flexible wing, deg
α_g	local angle of attack of rigid wing, deg
α_s	change in angle of attack caused by wing deflection
$\dot{\alpha} = \frac{1}{57.3}\frac{d\alpha}{dt}$,	radians per second
θ	angle of pitch, radians; angle of rotation of reference chord, deg
$\dot{\theta} = \frac{d\theta}{dt}$,	radians per second
θ/L	rotation of reference chord due to a unit concentrated load applied at reference station
e	distance between loading axis and assumed center-of-pressure axis, fraction of chord
ϕ_P	structural influence coefficients for angle-of-attack change due to unit concentrated loads applied along reference axis, deg/lb
ϕ_T	structural influence coefficients for angle-of-attack change due to unit torque applied parallel to free stream, deg/ft-lb
$\{\ \}$	column matrix
$[\ ]$	square matrix

$[^{0}]$ diagonal matrix

$[^{0}_{I}]$ diagonal matrix with nonzero elements equal to 1

$[I]$ square matrix with all elements equal to 1

$[\,I\,]$ row matrix with all elements equal to 1

MODELS AND TESTS

Models

A sketch of the models tested showing the pertinent dimensions is presented in figure 1. Photographs of the models are shown in figure 2. The fuselage was a curved body of revolution with a maximum diameter of 6.77 inches and a fineness ratio of 10. The fuselage ordinates are given in table I.

The three models tested were of similar construction except for the metal inlays in the wings. The wing geometry was as follows: aspect ratio 6.0, taper ratio 0.6, free-stream airfoil section NACA 65A009, and 45° angle of sweep of the quarter-chord line. The wing construction showing the inlays is presented in figure 3(a). The different inlays with their respective θ/L values were as follows: 0.064-inch-thick Inconel for model 1, with θ/L of -0.0075 degrees per pound; 0.032-inch-thick Inconel for model 2, with θ/L of -0.0112 degrees per pound; and 0.064-inch-thick 24 S-T aluminum alloy for model 3, with θ/L of -0.0224 degree per pound.

Directional stability was obtained for the models by the use of two vertical tails of 24 S-T aluminum. The tail plan form may be seen in the sketch of figure 1.

The models were equipped with four-channel telemeters which provided measurements of normal and longitudinal acceleration, total pressure, and angle of attack.

During the coasting portion of the flight, the models were disturbed in pitch by successive firing of eight pulse rockets. These pulse rockets were located in the fuselage in groups of four with their lines of thrust perpendicular to the plane of the wings. (See fig. 1.) The total impulse

of the pulse rockets used was about 6.1 pound-seconds and the thrust-time curve is approximately 120 sin 39.3t pound from zero time to 0.08 second.

TESTS

Structural influence coefficients were measured on test panels which reproduced the wing structure as closely as was possible. The influence coefficients ϕ_P for the angle-of-attack change were determined for loadings on the 25-percent-chord line, which will be referred to hereafter as the reference axis and for loadings on the 50-percent-chord line. A linear variation between the experimental influence coefficients obtained along the 25- and 50-percent-chord lines was assumed and the torsional coefficients ϕ_T were then calculated on this basis. Figure 4 shows the values of these coefficients for model 3, the most flexible of the series.

The models were launched at approximately 70° from the horizontal by means of a rail launcher (fig. 5). Model propulsion consisted of a 65-inch HVAR rocket motor as a booster with a $3\frac{1}{4}$-inch rocket motor sustainer. Atmospheric data were determined by radiosonde observations and trajectory and flight velocity were measured by an SCR-584 radar and a CW Doppler radar set, respectively.

The variations of dynamic pressure and Reynolds number with Mach number are shown in figures 6 and 7.

ANALYSIS

Inasmuch as the purpose of this analysis is to compare the results given by existing methods for the prediction of the effect of wing elasticity upon the rigid-wing lift-curve slope with experimental values, it would be well to state the primary methods which have been suggested.

There are two general approaches to the problem which might be termed the aerodynamic and the structural. In the aerodynamic approach, the structural aspects are not usually developed in detail and their effects are accounted for through assumed deflection curves whereas the main emphasis is placed on the aerodynamic considerations. Conversely, in the structural approach, the aerodynamic contribution is usually estimated by use of strip theory which, in some cases, includes a so-called tip correction, and the structure is investigated in detail.

If the equation representing the contribution of forces and moments at one station to the change in angle of attack at another station is written as

$$\alpha_s = \phi_P P + \phi_T ecP$$

it can be seen that the structural influence is manifested directly through the influence coefficients ϕ_P and ϕ_T; and the aerodynamic, through the loading P and the moment arm ec. Therefore, the two approaches may be discussed and appreciated through an investigation of these separate quantities ϕ_P and ϕ_T and P and ec along with their individual effects upon the lifting effectiveness of the wing.

Aerodynamic Approach

For this investigation, the change in angle of attack caused by the action of aerodynamic and inertia loads on a flexible wing structure is considered to be the sum of the torsional and bending contributions of the load distribution. The twisting effect is the result of the load distribution having a center-of-pressure axis displaced from the reference axis. The bending of the wing also effectively causes a rotation of the free-stream chord because the wing tends to bend and twist normal to the reference axis which is swept back at an angle to the free stream.

Various methods have been suggested to approximate the lift distribution on flexible sweptback wings. Some of the distributions which have either been used in the previous methods or appear applicable for use are as follows: Weissinger's simplified lifting-surface theory (refs. 4 and 5) and empirical methods based on this theory or on lifting-line theory (ref. 6) for subsonic speeds; linearized lifting-surface theory (ref. 2) for supersonic speeds; and strip theory with or without tip corrections for all speeds, as used in reference 3 and the calculations of reference 1.

The effect of these different assumed load distributions on the effective lift-curve slope ratio $C_{L_{\alpha_e}}/C_{L_{\alpha_r}}$, which is the ratio of the flexible-wing lift-curve slope to the rigid-wing lift-curve slope, can be determined by evaluating the effective lift produced by these distributions in conjunction with experimentally determined influence coefficients. The most convenient approach to the problem of representing the deflections and rotations of the wing structure appears to be in the form of influence coefficients. This method obviates the representation of the structural deformation as a series of assumed deflection modes.

The use of influence coefficients reduces the problem to the solution of a set of simultaneous equations; this procedure is facilitated by matrix notation.

Structural Approach

Experimentally determined influence coefficients are the most desirable but naturally assume the wing to be available for the necessary testing. When this is not the case, the structural behavior of the wing must be approximated.

The most frequently applied approximation is that based on simple beam theory where the wing is assumed to be cantilevered at an "effective root." The effective root was initially considered to be a line normal to the elastic axis passing through the intersection of the elastic axis and the fuselage chord. The elastic axis is usually considered to be the locus of the section shear centers without consideration of the effect of root restraint.

This method does not adequately represent the rigidity of the triangular portion of the wing formed by the wing root and the effective root. A truer representation is afforded if the effective root is moved outboard. The required amount of movement of the root is uncertain, inasmuch as the exact position can usually be determined only by experimentation or by a very detailed analysis of the wing structure. A good approximation to the position of the effective root is that formed by a line normal to the elastic axis passing through the intersection of the fuselage chord and the wing trailing edge. This concept is more fully explained in reference 7; however, the use of influence coefficients makes the consideration of the elastic axis unnecessary.

Approaches assuming specific deflection curves or those which are based on geometric or structural criteria are not discussed inasmuch as these wings are so constructed as to fit the necessary assumptions and, consequently, are no longer "arbitrary" wings.

Method Used in the Present Paper

Assumptions.- For the method used in this paper, the following assumptions are made:

(1) The total angle-of-attack change due to wing flexibility α_s is a result of wing bending and torsion, and these effects may be separated and treated individually.

(2) For the purpose of determining the load distribution, the wing is divided into a number of panels. The lift-curve slope of the panel is assumed to be that of the chord at the panel midpoint. The load on the panel is assumed to be a concentrated load acting at the intersection of the panel midchord and the center-of-pressure axis. This point is called a loading point. Figure 3(b) shows the division of the wing into the reference-panel areas and the positions of the loading and measuring stations as assumed for this analysis.

(3) The center-of-pressure axis is assumed to be at a constant percent of the chord. This assumption is maintained throughout the investigation; however, a means of treating those cases in which the center of pressure is not a constant percent of the chord is presented in the "Analysis" section.

(4) Aerodynamic induction effects are not considered after the initial load distribution has been assumed. Strip theory is used to calculate the lift caused by a structural deformation so that the changes in the lift on a reference station do not influence the lift on any other panel.

Development of the aeroelastic equation.- The method presented here is similar to that of reference 1 and is simplified by assuming constant-chord segments and not using integrating matrices. The basic equation for the contribution of the forces and moments at one station to the change in angle of attack at the same or another station is

$$\alpha_s = \phi_P P + \phi_T T \tag{1}$$

where P is the distributed load along the wing span and T is the twisting moment produced by the displacement of P from the elastic axis or from the reference axis used for the determination of ϕ_P.

$$T = ecP$$

therefore,

$$\alpha_s = \left(\phi_P + ec\phi_T\right)P \tag{2}$$

Since the structural characteristics of the wing are represented as influence coefficients, the loading P must be expressed in a corresponding form. If the influence coefficients are assumed known for a

set of reference stations, the effective load must also be known for these stations which are taken at the odd tenths of the exposed semispan. According to assumption (2), the effective load on a panel can be assumed to act through a point; in this case, the point is the reference station. Simultaneous considerations of all the loads acting on all the stations resolves the problem into the following set of simultaneous equations:

$$\left.\begin{aligned}
\alpha_{s_0} &= P_0(\phi_P + ec\phi_T)_{00} + P_1(\phi_P + ec\phi_T)_{01} + P_3(\phi_P + ec\phi_T)_{03} + \\
&\quad P_5(\phi_P + ec\phi_T)_{05} + \cdots \\
\alpha_{s_1} &= P_0(\phi_P + ec\phi_T)_{10} + \cdots \\
\alpha_{s_3} &= P_0(\phi_P + ec\phi_T)_{30} + \cdots \\
\alpha_{s_5} &= P_0(\phi_P + ec\phi_T)_{50} + \cdots + P_3(\phi_P + ec\phi_T)_{53} + \cdots \\
\alpha_{s_7} &= P_0(\phi_P + ec\phi_T)_{70} + \cdots \\
\alpha_{s_9} &= P_0(\phi_P + ec\phi_T)_{90} + \cdots
\end{aligned}\right\} \quad (3)$$

The subscripts of α_s refer to the spanwise station, in tenths of the exposed semispan, at which the change in angle of attack is measured. The subscript of P refers to the exposed semispan station, also in tenths at which the load is applied. The first subscript of the combined influence coefficients $(\phi_P + ec\phi_T)$ refers to the spanwise station at which the change in angle of attack was measured and the second that at which the load was applied. For example, $(\phi_P + ec\phi_T)_{53}$ in the equation for α_{s_5} means the rotation of the chord is measured at station 5 and is due to a load applied at station 3. The amount of rotation contributed by this load P_3 to α_{s_5} is equal in magnitude to $P_3(\phi_P + ec\phi_T)_{53}$.

The above set of simultaneous equations and its subsequent manipulations may be most readily handled by matrix notation.

The equations leading up to equation (3) when rewritten in matrix form become

$$\{\alpha_s\} = [\phi_P]\{P\} + [\phi_T]\{T\} \quad (4)$$

The twisting moment $\{T\} = [ec]\{P\}$

Hence,

$$\left\{\alpha_s\right\} = \left[\left[\varphi_P\right] + \left[\varphi_T\right]\left[e^{\circ}_{c}\right]\right]\left\{P\right\} \tag{5}$$

The load P on any reference panel equals the lift on the panel minus the effect of wing inertia

$$P_{panel} = L_{panel} - a_{n_{panel}} W_{panel} \tag{6}$$

where a_n is in g units, and

$$a_n = \frac{N}{W} \approx \frac{L_{total}}{W_{total}}. \tag{7}$$

The lift on an elastically deformed wing is

$$L = 2q\int_0^{b/2} cc_{l_\alpha}\bar{\alpha}\, dy$$

which in matrix notation is

$$L = 2q\left[I\right]\left[\Delta s^{\circ}\right]\left[c^{\circ}_{l_\alpha}\right]\left\{\bar{\alpha}\right\}$$

or

$$L = 2qC_{L_{\alpha_r}}\left[I\right]\left[\Delta s^{\circ}\right]\left[\frac{c^{\circ}_{l_\alpha}}{C_{L_{\alpha_r}}}\right]\left\{\bar{\alpha}\right\} \tag{8}$$

In equation (8) and the following derivation, the matrix $\left[\frac{c^{\circ}_{l_\alpha}}{C_{L_{\alpha_r}}}\right]$ is used to represent the different types of loading distributions (simplified subsonic lifting surface theory, etc.). For strip theory

$\left[\frac{c_{l_\alpha}}{C_{L_{\alpha_r}}}\right] = K\left[I\right]$ where K represents an overall reduction in lift. If this factor is ignored, a procedure which is justified to a certain extent at supersonic speeds, K is equal to one.

If equations (7) and (8) are substituted into equation (6), the following expression is obtained:

$$\left\{P\right\} = qC_{L_{\alpha_r}}\left[\Delta s\right]\left[\frac{c_{l_\alpha}}{C_{L_{\alpha_r}}}\right]\left\{\bar{\alpha}\right\} - 2qC_{L_{\alpha_r}}\left(\left[I\right]\left[\Delta s\right]\left[\frac{c_{l_\alpha}}{C_{L_{\alpha_r}}}\right]\left\{\bar{\alpha}\right\}\right)\left\{\frac{w}{W}\right\}$$

For the purpose of this derivation, the last term in this equation is in an inconvenient form; the desired form, which consists of a square matrix multiplied by a column matrix of the local angle-of-attack values, can be obtained by a device used in reference 8, since

$$\left(\left[I\right]\left[\Delta s\right]\left[\frac{c_{l_\alpha}}{C_{L_{\alpha_r}}}\right]\left\{\bar{\alpha}\right\}\right)\left\{\frac{w}{W}\right\} = \left\{\frac{w}{W}\right\}\left(\left[I\right]\left[\Delta s\right]\left[\frac{c_{l_\alpha}}{C_{L_{\alpha_r}}}\right]\left\{\bar{\alpha}\right\}\right)$$

and

$$\left\{\frac{w}{W}\right\}\left[I\right] = \left[\frac{w}{W}\right]$$

The previous equation for $\left\{P\right\}$ can be rewritten as

$$\left\{P\right\} = qC_{L_{\alpha_r}}\left[\Delta s\right]\left[\frac{c_{l_\alpha}}{C_{L_{\alpha_r}}}\right]\left\{\bar{\alpha}\right\} - 2qC_{L_{\alpha_r}}\left[\frac{w}{W}\right]\left[\Delta s\right]\left[\frac{c_{l_\alpha}}{C_{L_{\alpha_r}}}\right]\left\{\bar{\alpha}\right\}$$

which becomes

$$\left\{P\right\} = qC_{L_{\alpha_r}}\left[\left[I\right] - 2\left[\frac{w}{W}\right]\right]\left[\Delta s\right]\left[\frac{c_{l_\alpha}}{C_{L_{\alpha_r}}}\right]\left\{\bar{\alpha}\right\}$$

The aeroelastic equation is then obtained by substituting this expression for $\{P\}$ into equation (5); the resulting equation is

$$\{\alpha_s\} = qC_{L_{\alpha_r}}\left[[\varphi_P] + [\varphi_T]\left[\overset{\circ}{ec}\right]\right]\left[\left[\overset{\circ}{I}\right] - 2\left[\frac{w}{W}\right]\right]\left[\overset{\circ}{\Delta s}\right]\left[\frac{\overset{\circ}{c_{l_\alpha}}}{C_{L_{\alpha_r}}}\right]\{\bar{\alpha}\}$$

Structural influence coefficients were determined experimentally. The ratio between corresponding influence coefficients of the reference wing and another wing of similar construction and plan form is constant and equal to the reference θ/L values of each wing where the parameter θ/L refers to a rotation of the streamwise chord at a reference station through an angle θ due to a concentrated load L applied at the same or a second reference station. This ratio may be expressed as

$$k \equiv \frac{\theta/L}{(\theta/L)_{\text{reference}}}$$

where $(\theta/L)_{\text{reference}}$ refers to the wing for which the influence coefficients were determined. This ratio may be introduced into equation (9) as follows:

$$\{\alpha_s\} = qC_{L_{\alpha_r}}k\left[[\varphi_P] + [\varphi_T]\left[\overset{\circ}{ec}\right]\right]\left[\left[\overset{\circ}{I}\right] - 2\left[\frac{w}{W}\right]\right]\left[\overset{\circ}{\Delta s}\right]\left[\frac{\overset{\circ}{c_{l_\alpha}}}{C_{L_{\alpha_r}}}\right]\{\bar{\alpha}\}$$

and since, by definition,

$$\{\bar{\alpha}\} = \{\alpha_g\} + \{\alpha_s\}$$

the solution of the equation is

$$\{\bar{\alpha}\} = \left[\left[\overset{\circ}{I}\right] - qC_{L_{\alpha_r}}k\left[[\varphi_P] + [\varphi_T]\left[\overset{\circ}{ec}\right]\right]\left[\left[\overset{\circ}{I}\right] - 2\left[\frac{w}{W}\right]\right]\left[\overset{\circ}{\Delta s}\right]\left[\frac{\overset{\circ}{c_{l_\alpha}}}{C_{L_{\alpha_r}}}\right]\right]^{-1}\{\alpha_g\} \tag{10}$$

Equation (10) may be solved in a number of ways with Crout's method of reference 9, probably the most suitable method for manual computing machines.

If the center of pressure is located at a constant percent of the chord, the matrix $[\varphi_T]\ [\overset{\circ}{ec}]$ in equation (10) can be replaced by $e[\varphi_T]\ [\overset{\circ}{c}]$, and if, in addition, strip theory is used with a factor K equal to 1, equation (10) becomes

$$\{\bar{\alpha}\} = \left[[\overset{\circ}{I}] - qC_{L_{\alpha_r}} k\left[[\varphi_P] + e[\varphi_T][\overset{\circ}{c}]\right]\left[[\overset{\circ}{I}] - 2\left[\frac{w}{W}\right][\overset{\circ}{\Delta s}]\right]^{-1}\right]\{\alpha_g\} \tag{11}$$

If the twisting effect is neglected this equation is further simplified to

$$\{\bar{\alpha}\} = \left[[\overset{\circ}{I}] - qC_{L_{\alpha_r}} k[\varphi_P]\left[[\overset{\circ}{I}] - 2\left[\frac{w}{W}\right][\overset{\circ}{\Delta s}]\right]^{-1}\right]\{\alpha_g\} \tag{11a}$$

and if the inertia effects are neglected and the values e are assumed constant along the span, equation (11) becomes

$$\{\bar{\alpha}\} = \left[[\overset{\circ}{I}] - qC_{L_{\alpha_r}} k\left[[\varphi_P] + e[\varphi_T][\overset{\circ}{c}]\right][\overset{\circ}{\Delta s}]\left[\frac{\overset{\circ}{c_{l_\alpha}}}{C_{L_{\alpha_r}}}\right]^{-1}\right]\{\alpha_g\} \tag{12}$$

The effective lift-curve slope $C_{L_{\alpha_e}}$ may be defined as

$$C_{L_{\alpha_e}} = \frac{L}{qS\alpha_g}$$

where α_g is assumed constant along the span.

Equation (8) can be written as

$$L = C_{L_{\alpha_e}} qS\alpha_g = 2qC_{L_{\alpha_r}}[I][\overset{\circ}{\Delta s}]\left[\frac{\overset{\circ}{c_{l_\alpha}}}{C_{L_{\alpha_r}}}\right]\{\bar{\alpha}\}$$

so that the effective lift ratio is

$$\frac{C_{L_{\alpha_e}}}{C_{L_{\alpha_r}}} = \frac{2}{S}\frac{1}{\alpha_g}\left[I\right]\left[\overset{o}{\Delta s}\right]\left[\frac{\overset{o}{c_l}_{\alpha}}{C_{L_{\alpha_r}}}\right]\left\{\bar{\alpha}\right\} \tag{13}$$

The effects of substituting a strip-theory distribution for a more exact distribution, of neglecting the effect of the twisting contribution, and of neglecting the effect of the inertia forces are investigated in the illustrative example.

ILLUSTRATIVE EXAMPLE

In order to illustrate the differences in the effective lift ratio $C_{L_{\alpha_e}}/C_{L_{\alpha_r}}$ for different assumed load distributions and center-of-pressure positions, the load-flexibility parameter $qC_{L_{\alpha_r}}k$ is assumed to be sufficiently large to cause a loss of about forty percent in the lifting effectiveness of the wing.

The experimental influence coefficients for the wing with the 0.064-inch aluminum-alloy inlays are

$$\left[\phi_P\right] = \begin{array}{c} \\ \text{Measuring Stations} \\ \\ 0 \\ 1 \\ 3 \\ 5 \\ 7 \\ 9 \end{array} \begin{array}{c} \text{Loading Stations} \\ \begin{array}{cccccc} 0 & 1 & 3 & 5 & 7 & 9 \end{array} \\ \left[\begin{array}{cccccc} 0 & 0 & 0 & 0 & 0 & 0 \\ 0 & 0 & -0.0006 & -0.0014 & -0.0024 & -0.0044 \\ 0 & 0 & -0.0008 & -0.0035 & -0.0066 & -0.0124 \\ 0 & 0 & -0.0015 & -0.0045 & -0.0096 & -0.0196 \\ 0 & 0 & -0.0012 & -0.0046 & -0.0106 & -0.0222 \\ 0 & 0 & -0.0011 & -0.0041 & -0.0104 & -0.0224 \end{array}\right] \end{array} \frac{\text{degrees}}{\text{pound}}$$

[redacted]

$$\left[\phi_T\right] = \begin{bmatrix} 0 & 0 & 0 & 0 & 0 & 0 \\ 0 & 0 & 0.0005 & 0.0012 & 0.0021 & 0.0039 \\ 0 & 0 & 0.0008 & 0.0033 & 0.0063 & 0.0118 \\ 0 & 0 & 0.0016 & 0.0047 & 0.0099 & 0.0203 \\ 0 & 0 & 0.0014 & 0.0052 & 0.0121 & 0.0252 \\ 0 & 0 & 0.0014 & 0.0051 & 0.0131 & 0.0281 \end{bmatrix} \frac{\text{degrees}}{\text{foot-pound}}$$

Equation (10) is solved by using a rigid-wing lift distribution calculated from reference 5. Equation (11) which utilizes strip theory is also solved and the different results are compared to determine the effect of the load distribution.

The expression for $\left[\frac{c_{l_\alpha}^{o}}{C_{L_{\alpha_r}}}\right]$ according to reference 5 for a Mach number of 0.8 is

$$\left[\frac{c_{l_\alpha}^{o}}{C_{L_{\alpha_r}}}\right] = \begin{bmatrix} 0.842 & 0 & 0 & 0 & 0 & 0 \\ 0 & 0.922 & 0 & 0 & 0 & 0 \\ 0 & 0 & 1.061 & 0 & 0 & 0 \\ 0 & 0 & 0 & 1.155 & 0 & 0 \\ 0 & 0 & 0 & 0 & 1.160 & 0 \\ 0 & 0 & 0 & 0 & 0 & 0.920 \end{bmatrix}$$

For this wing with 0.064-inch aluminum-alloy inlays, the weight distribution is given by

$$\left[\frac{w}{W}\right] = \begin{bmatrix} * & * & * & * & * & * \\ 0.0345 & 0.0345 & 0.0345 & 0.0345 & 0.0345 & 0.0345 \\ 0.0301 & 0.0301 & 0.0301 & 0.0301 & 0.0301 & 0.0345 \\ 0.0260 & 0.0260 & 0.0260 & 0.0260 & 0.0260 & 0.0260 \\ 0.0223 & 0.0223 & 0.0223 & 0.0223 & 0.0223 & 0.0223 \\ 0.0188 & 0.0188 & 0.0188 & 0.0188 & 0.0188 & 0.0188 \end{bmatrix}$$

(The number denoted by an asterisk is unnecessary since the multiplying elements in the influence-coefficient matrices are zero.) The pertinent geometric characteristics are given by

$$\left[\overset{o}{\Delta s}\right] = \begin{bmatrix} 0.320 & 0 & 0 & 0 & 0 & 0 \\ 0 & 0.381 & 0 & 0 & 0 & 0 \\ 0 & 0 & 0.352 & 0 & 0 & 0 \\ 0 & 0 & 0 & 0.323 & 0 & 0 \\ 0 & 0 & 0 & 0 & 0.295 & 0 \\ 0 & 0 & 0 & 0 & 0 & 0.270 \end{bmatrix}$$

$$\left[\overset{o}{c}\right] = \begin{bmatrix} 0.976 & 0 & 0 & 0 & 0 & 0 \\ 0 & 0.912 & 0 & 0 & 0 & 0 \\ 0 & 0 & 0.843 & 0 & 0 & 0 \\ 0 & 0 & 0 & 0.774 & 0 & 0 \\ 0 & 0 & 0 & 0 & 0.706 & 0 \\ 0 & 0 & 0 & 0 & 0 & 0.638 \end{bmatrix}$$

The load-flexibility parameter $C_{L_{\alpha r}} qk$ is assumed to be 10,000 and the rigid-wing angle of attack α_g is assumed constant at 1° along the span.

The center-of-pressure axis is assumed at the 0.25-chord line, which is the reference axis ϕ_P.

Solution of equation (10) using the above values yields the resultant load distribution $\left\{\bar{\alpha}\right\}$. Substituting this value into equation (13) yields a value of $\frac{C_{L_{\alpha_e}}}{C_{L_{\alpha_r}}}$ of 0.646 for this case.

Changing the load distribution from that of reference 5 to a strip-theory distribution, for the same conditions, yields a value of $\frac{C_{L_{\alpha_e}}}{C_{L_{\alpha_r}}}$ of 0.652, a change of less than 1 percent for this case of heavy wing loading.

If the second example, that using strip theory, is changed by assuming the center-of-pressure axis to be on the 0.50-chord line rather than the 0.25-chord line, a comparison may be made to determine the effect of center-of-pressure position for this case.

Changing only the value of e in equation (10) and solving the resulting equation gives a value of $\frac{C_{L_{\alpha_e}}}{C_{L_{\alpha_r}}}$ of 0.684 or about 3 percent difference from the previous case for the 0.25-chord loading.

RESULTS AND DISCUSSION

Figures 8 and 9 show the results of the flight tests of the three models. The procedure used in reducing the data from the telemeter records and radar observations to the final forms as presented in the figures is explained in reference 10.

In figure 8 the experimental values of C_{L_α} against Mach number are presented. Figure 10 shows the extrapolation of C_{L_α} to obtain the rigid-wing values. Figure 9 shows the variation of $C_{m_{\dot{\alpha}}} + C_{m_q}$ with Mach number, all models having the same center-of-gravity positions. The experimental values of the pitching-moment-curve slope are not presented

in this paper because the method of determination used assumes a linear slope of the pitching-moment angle-of-attack curve throughout the test range. Previous investigations have shown the pitching-moment angle-of-attack curve for this wing to be nonlinear at small positive and negative values of the angle of attack.

The curve of the effective-lift ratio $C_{L_{\alpha_e}}/C_{L_{\alpha_r}}$ against the load-flexibility parameter $C_{L_{\alpha_r}}qk$ is shown in figure 11. Here the results of a strip-theory load distribution calculated by equations (11) and (13) of the analysis section have been presented with center-of-pressure positions of 0.25-percent and 0.50-percent chord. If these two center-of-pressure positions are assumed to be the boundaries of the forward and rearward center-of-pressure movement, then most of the experimental points fall within these two limits. Those which fall outside the limits are possibly in error due to the experimental accuracy, the inability to extrapolate to the exact rigid-wing lift-curve slopes, or a combination of the two coupled with the accepted error arising from the approximate methods used to calculate the limits.

The results of comparing the effective lifting characteristics of this sweptback wing as predicted by approximate methods with the experimental values should not be accepted for all sweptback wings unless allowances are made for the aspect ratio. It is believed that the results do show that these approximate approaches are sufficient to predict the flexible-wing lift-curve slope of wings having an aspect ratio of 6 or higher. Reference 11 shows that a similar approach which uses influence coefficients and strip theory predicts the elastic lift of a 45° sweptback wing of aspect ratio 4 with a good degree of accuracy.

The differences between the values obtained by using either strip-theory or a more exact approximation for the rigid-wing lift distribution are small, about 1 percent where the greatest measured loss in lift was recorded. Inasmuch as the rigid-wing lift-curve slope can not always be determined with any more accuracy, it appears that strip theory would suffice for most of the cases encountered in practice.

For this wing of 45° sweepback and aspect ratio 6.0, the data indicate that the primary contribution to the twist of the wing is that of bending. When the center of pressure is assumed to be the 50-percent-chord line rather than the 25-percent-chord line the difference is only 3 percent for the worst loading condition. In practice, it is unusual if the rigid-wing lift-curve slope is known to any better accuracy.

[redacted]

CONCLUDING REMARKS

The results of the flight tests of three similar models with varying degrees of wing flexibility have been presented. These experimental values of the lift-curve slopes have been compared with the results calculated by a general method for the prediction of the lifting effectiveness of flexible sweptback wings. The effects of changes in the assumed load distributions and centers of pressure have been investigated also.

The results of the comparisons indicate that the effect of changing either the load distribution or the center of pressure is small, about 1 percent and 3 percent, respectively, for the cases of rigid-wing lift distributions investigated in the illustrative example.

The values of the effective lift-slope ratio as predicted by an assumed strip theory load distribution coupled with experimentally determined structural influence coefficients show good agreement with the experimental results. The agreement between the predicted and experimental values is within the accuracy with which the rigid-wing lift-curve slope can usually be determined in practice.

Langley Aeronautical Laboratory
National Advisory Committee for Aeronautics
Langley Field, Va., February 15, 1954.

REFERENCES

1. Diederich, Franklin W.: Calculation of the Aerodynamic Loading of Flexible Wings of Arbitrary Plan Form and Stiffness. NACA Rep. 1000, 1950. (Supersedes NACA TN 1876).

2. Frick, C. W., and Chubb, R. S.: The Longitudinal Stability of Elastic Swept Wings at Supersonic Speed. NACA Rep. 965, 1950. (Supersedes NACA TN 1811.)

3. Miles, John W.: A Formulation of the Aeroelastic Problem for a Swept Wing. Jour. Aero. Sci., vol 16, no. 8, Aug. 1949, pp. 477-490.

4. Skoog, Richard B., and Brown, Harvey H.: A Method for the Determination of the Spanwise Load Distribution of a Flexible Swept Wing at Subsonic Speeds. NACA TN 2222, 1951.

5. De Young, John, and Harper, Charles W.: Theoretical Symmetric Span Loading at Subsonic Speeds for Wings Having Arbitrary Plan Form. NACA Rep. 921, 1948.

6. Sivells, James C.: An Improved Approximate Method for Calculating Lift Distributions Due to Twist. NACA TN 2282, 1951.

7. Zender, George W., and Brooks, William A., Jr.: An Approximate Method of Calculating the Deformations of Wings Having Swept, M or W, Λ, and Swept-Tip Plan Forms. NACA TN 2978, 1953.

8. Diederich, Franklin W.: Calculation of the Lateral Control of Swept and Unswept Flexible Wings of Arbitrary Stiffness. NACA Rep. 1024, 1951.

9. Crout, Prescott D.: A Short Method for Evaluating Determinants and Solving Systems of Linear Equations with Real or Complex Coefficients. Trans. Am. Inst. Elec. Eng., vol 60, 1941, pp. 1235-1240.

10. Gillis, Clarence T., Peck, Robert F., and Vitale, A. James.: Preliminary Results From a Free-Flight Investigation at Transonic and Supersonic Speeds of the Longitudinal Stability and Control Characteristics of an Airplane Configuration With a Thin Straight Wing of Aspect Ratio 3. NACA RM L9K25A, 1950.

11. Vitale, A. James: Effects of Wing Elasticity on the Aerodynamic Characteristics of an Airplane Configuration Having 45° Sweptback Wings As Obtained From Free-Flight Rocket-Model Tests at Transonic Speeds. NACA RM L52L30, 1953.

TABLE I

BODY COORDINATES

x, in.	r, in.
0	0
1.00	.342
2.00	.578
4.00	.964
6.00	1.290
8.00	1.577
12.00	2.074
16.00	2.472
20.00	2.773
22.00	2.892
22.75	2.933
24.00	2.993
28.00	3.146
32.00	3.250
36.00	3.314
40.00	3.334
44.00	3.304
48.00	3.219
52.00	3.074
56.00	2.813
60.00	2.658
64.00	2.450
66.70	2.305
67.70	2.250

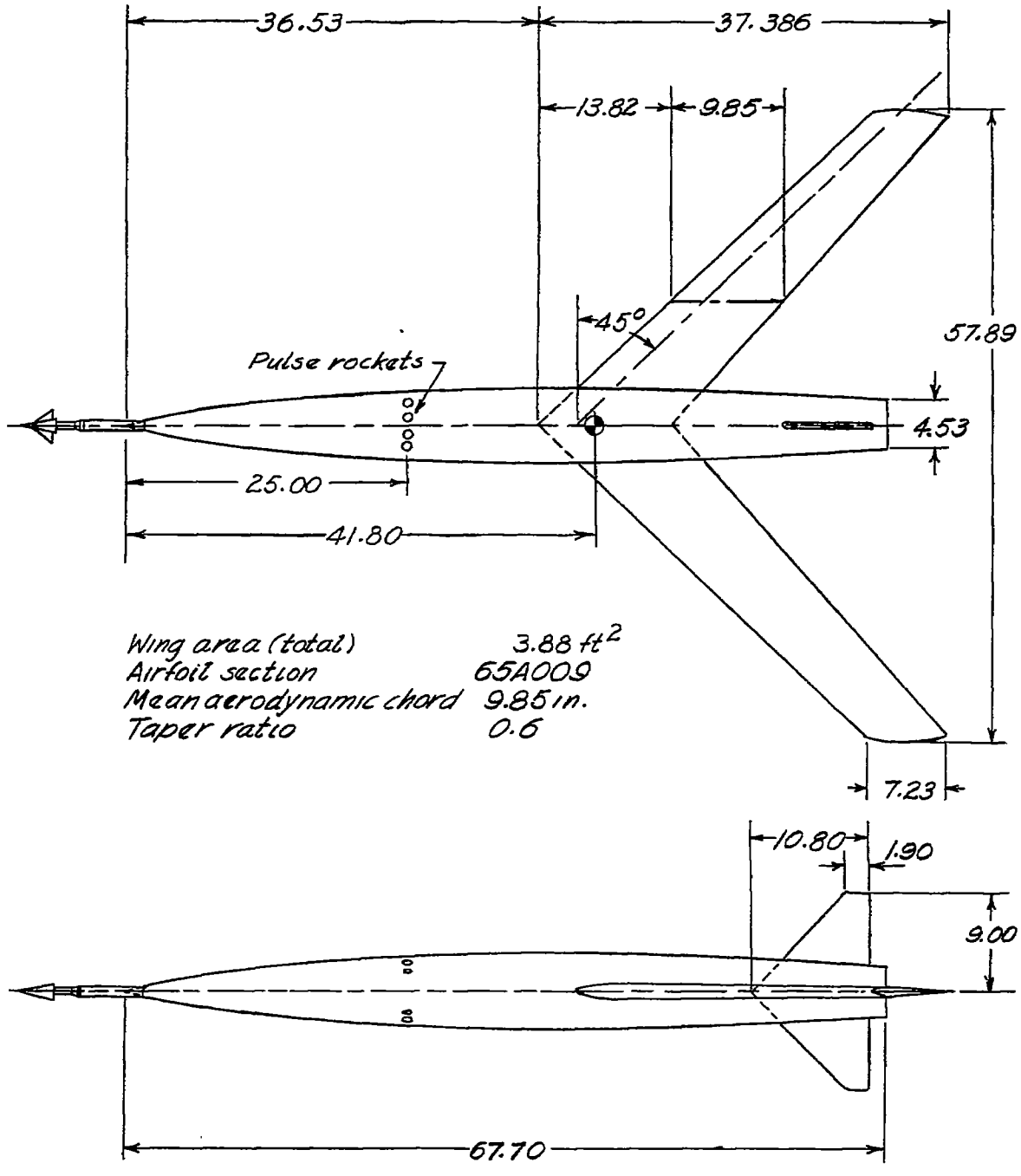

Figure 1.- General arrangement of models tested. All dimensions are in inches.

L-77687.1

(a) Top view.

Figure 2.- Photograph of model configuration.

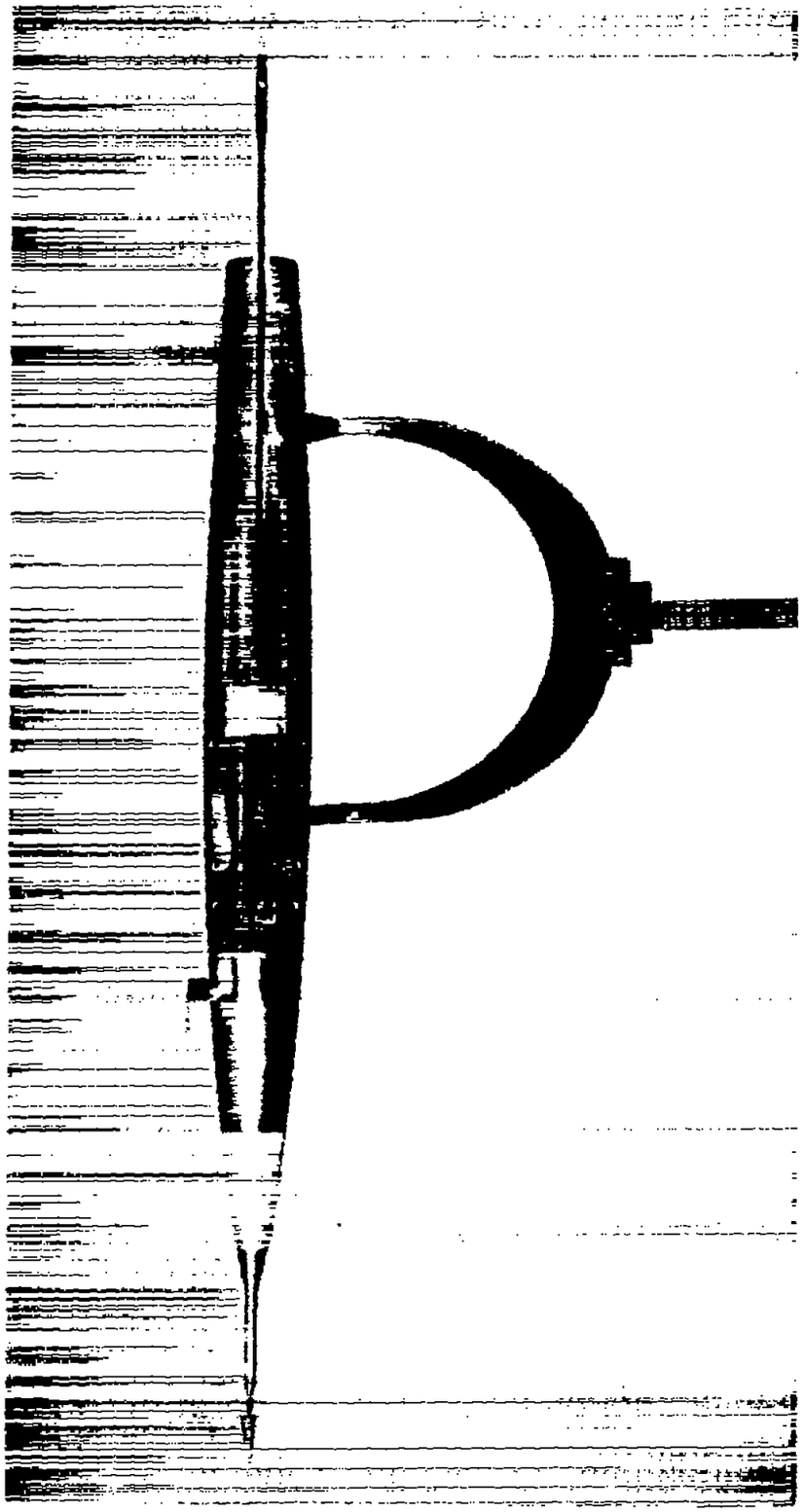

L-77688.1

(b) Side view.

Figure 2.- Concluded.

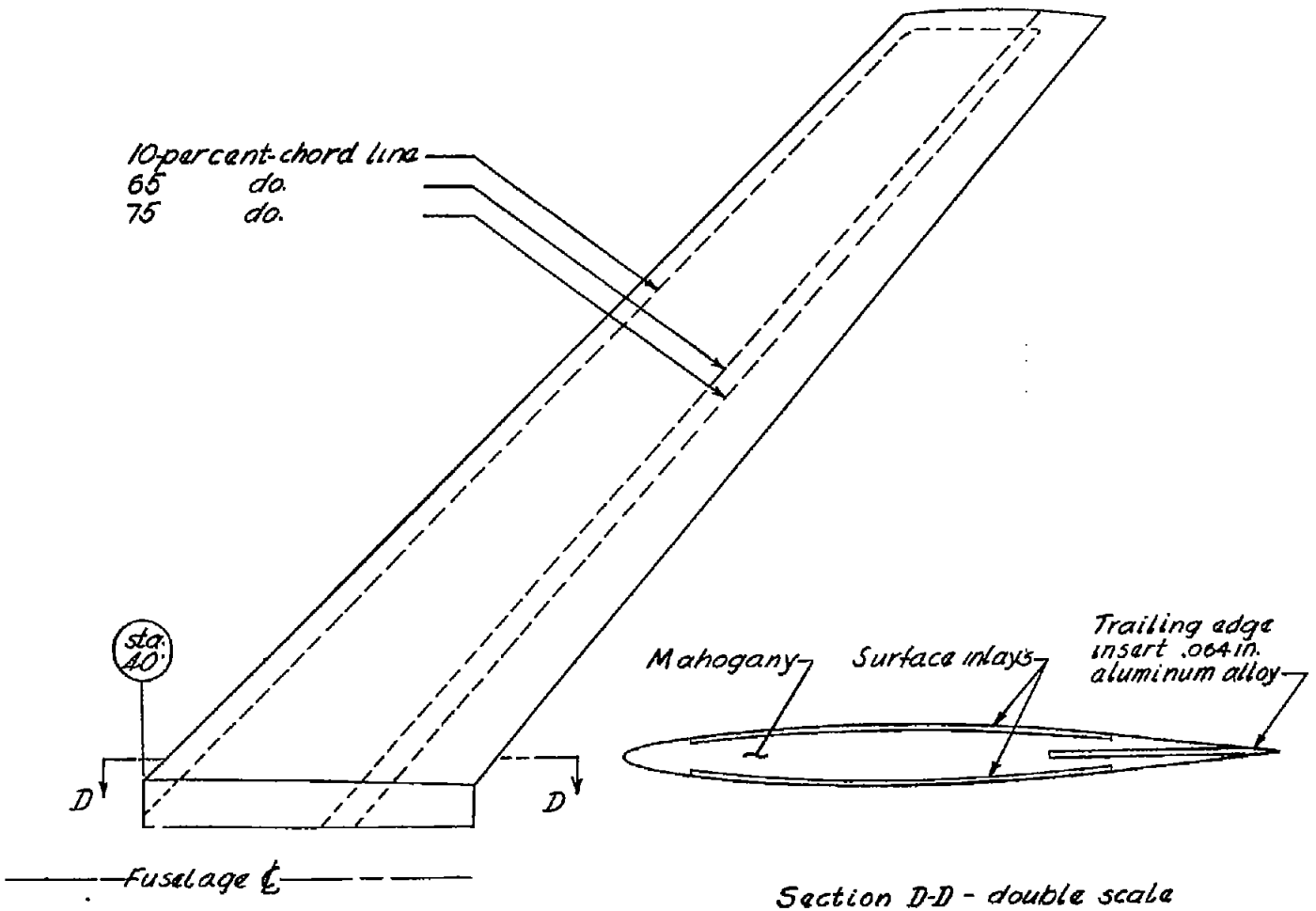

(a) Sketch of model wing showing wing construction.

Figure 3.- Wing construction and locations of loading and measuring stations for test wing.

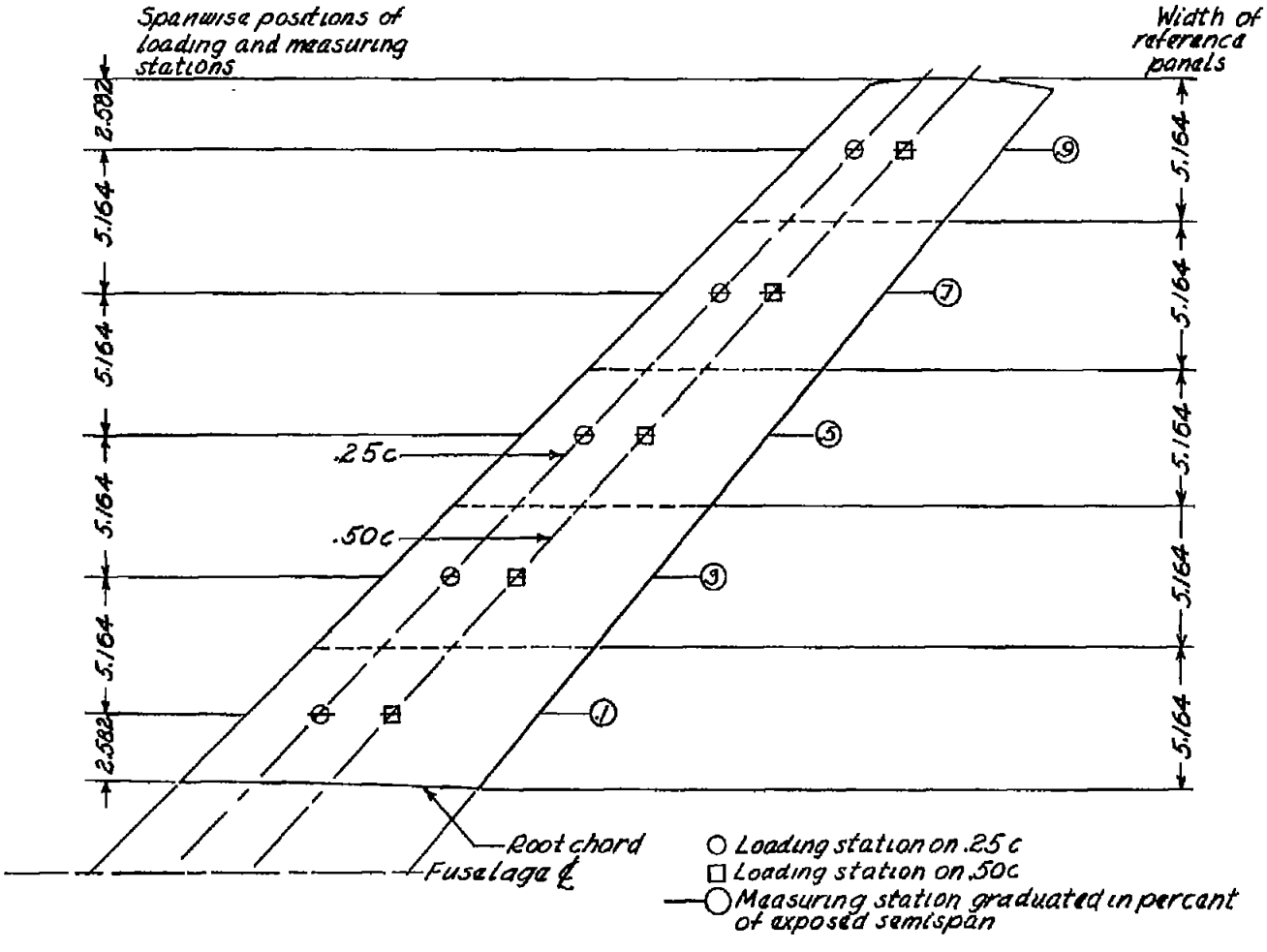

(b) Division of wing into reference panels and positions of measuring and loading stations. All dimensions are in inches.

Figure 3.- Concluded.

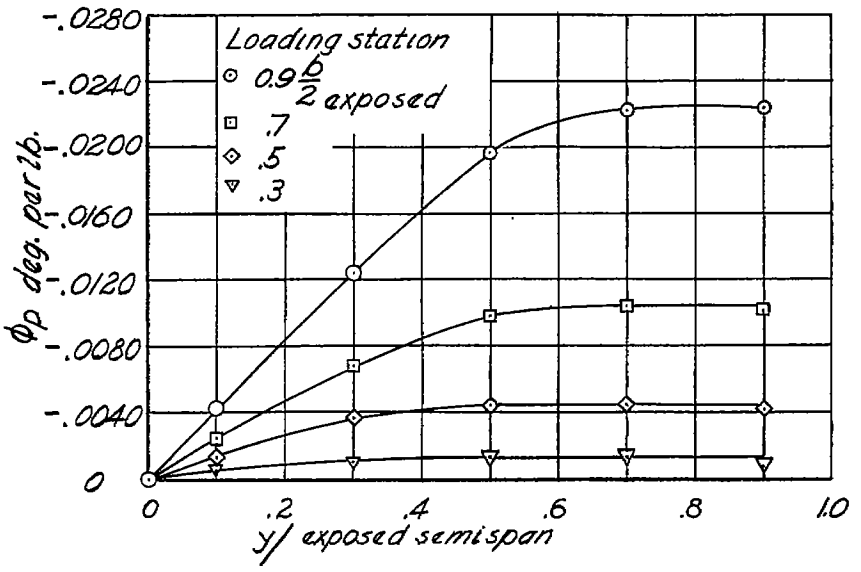

(a) Influence coefficients due to bending of reference axis.

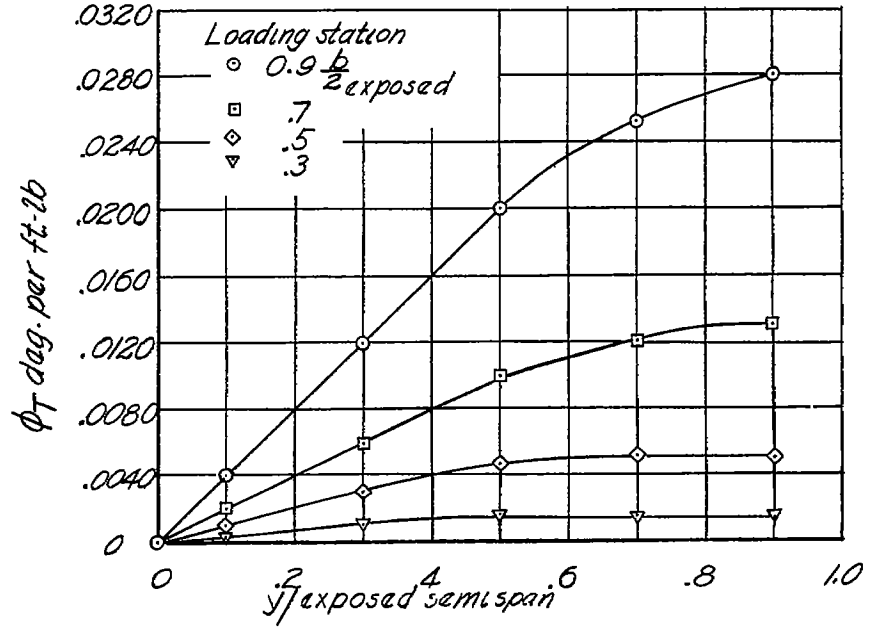

(b) Influence coefficients due to twist about the reference axis.

Figure 4.- Experimentally determined structural influence coefficients for model 3.

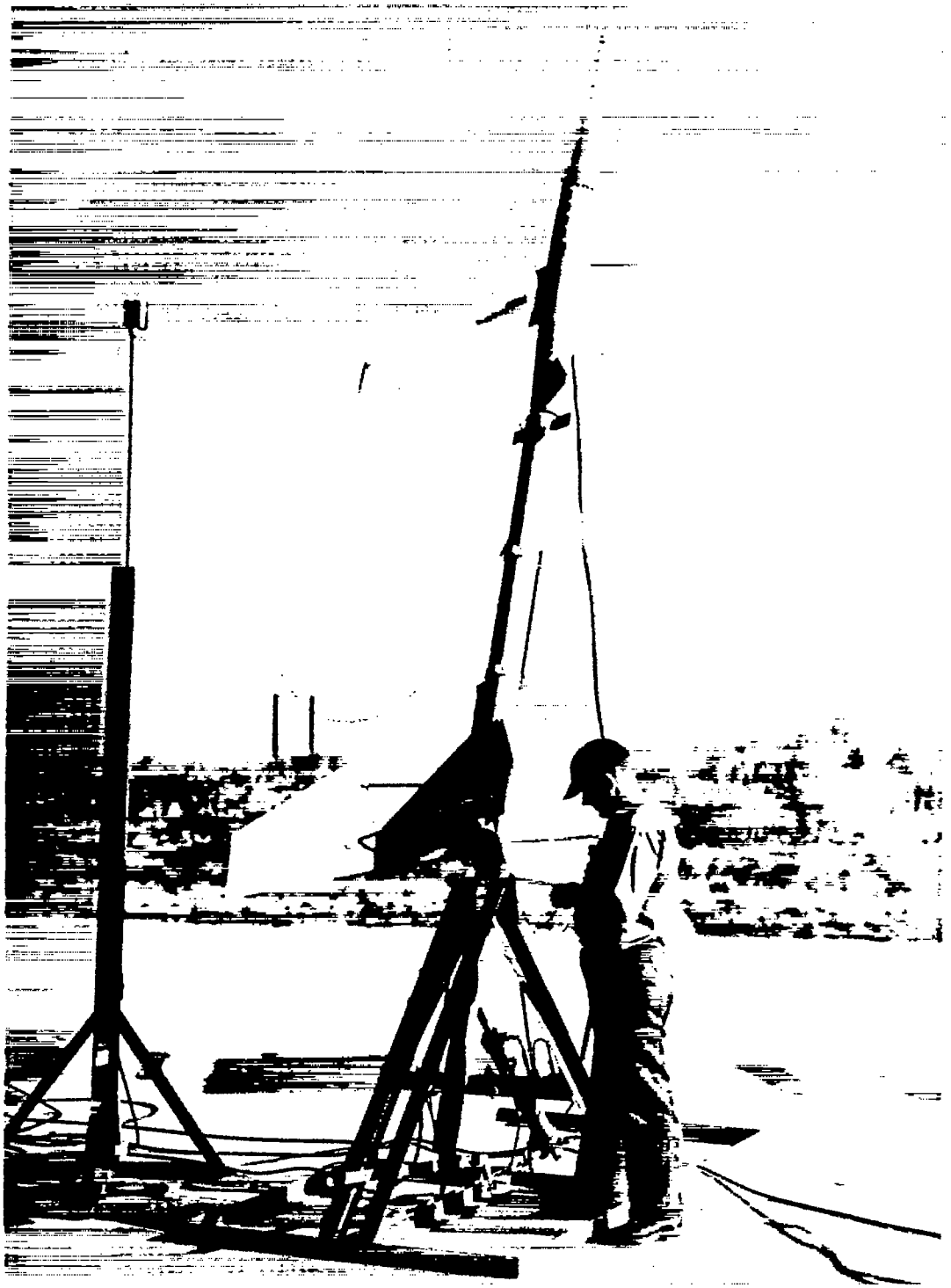

L-78079.1

Figure 5.- Model on launcher.

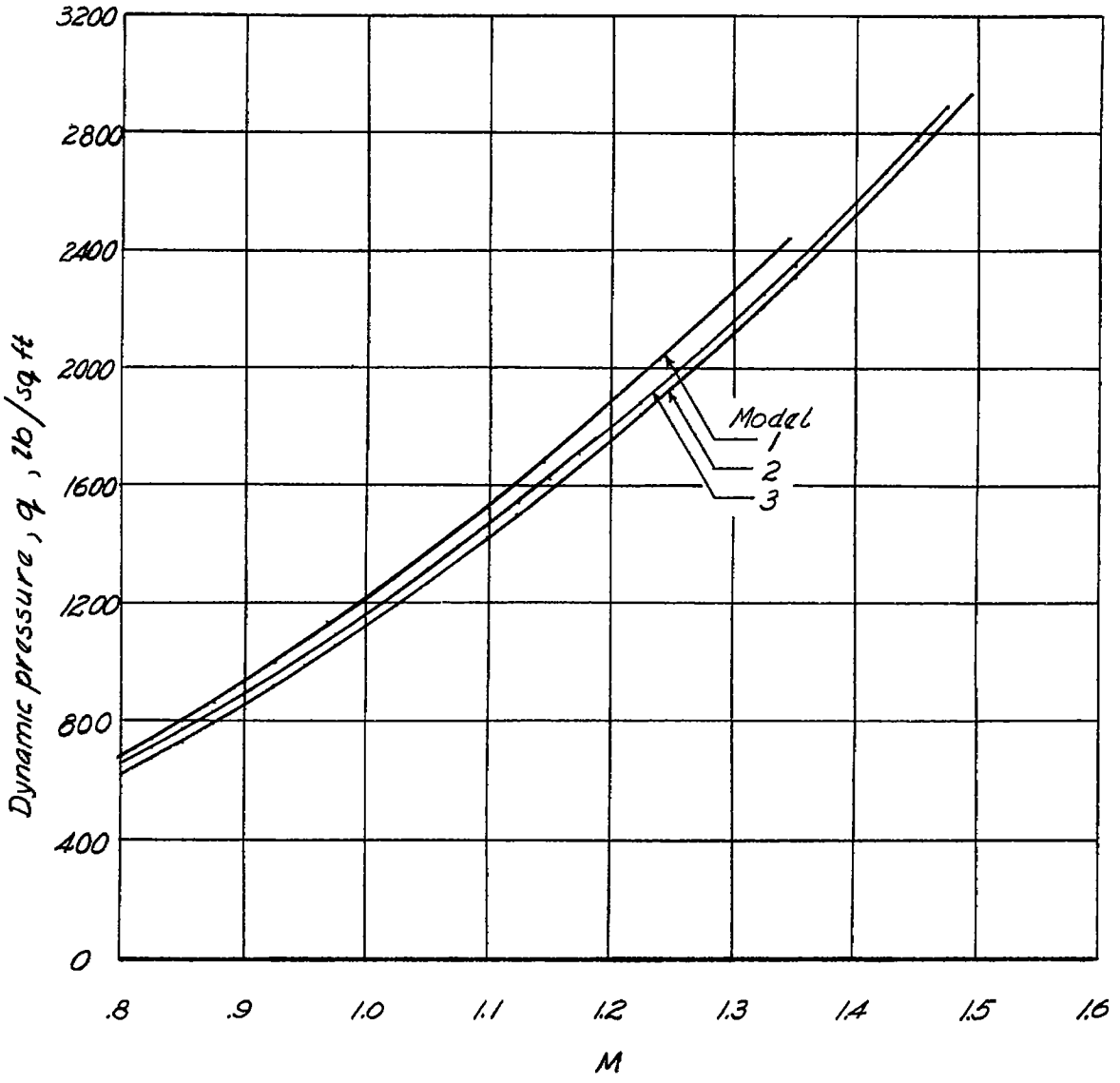

Figure 6.- Variation of dynamic pressure with Mach number.

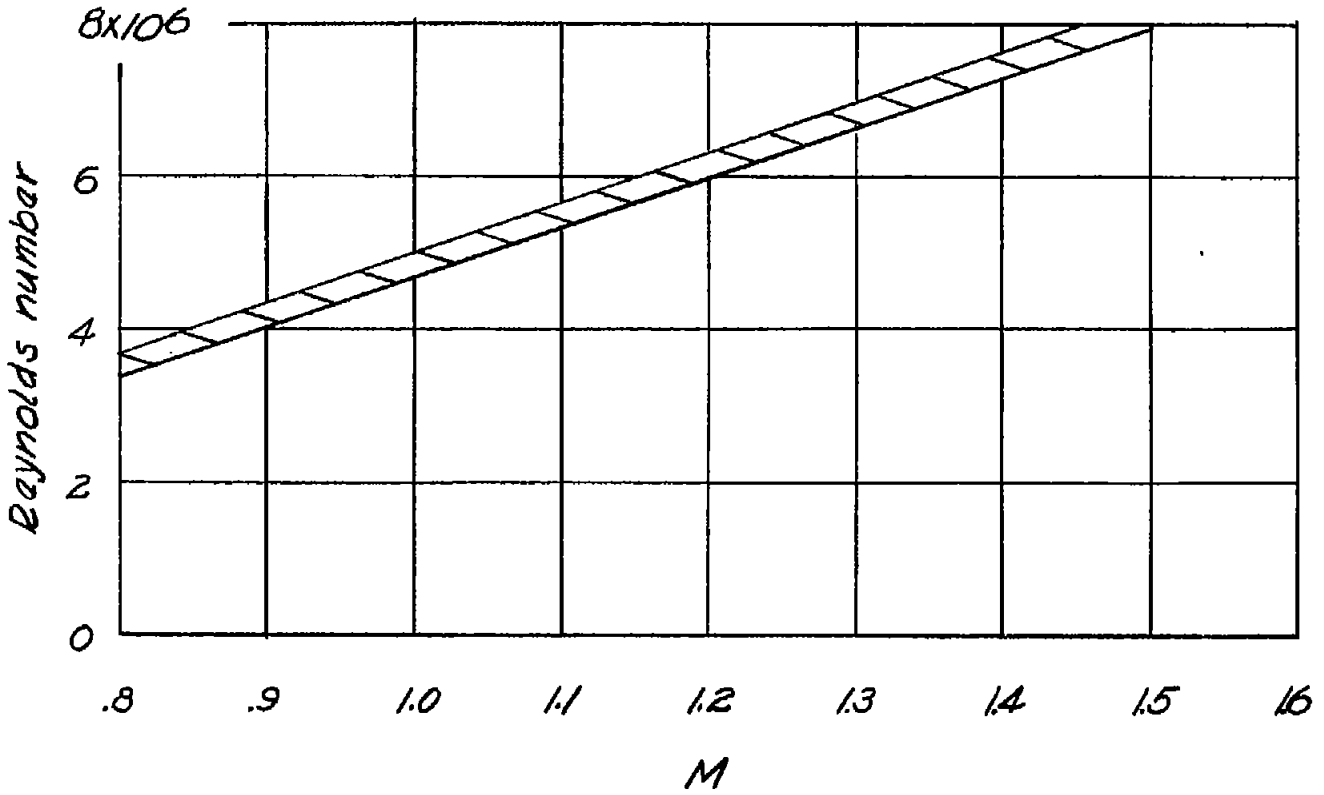

Figure 7.- Variation of Reynolds number with Mach number.

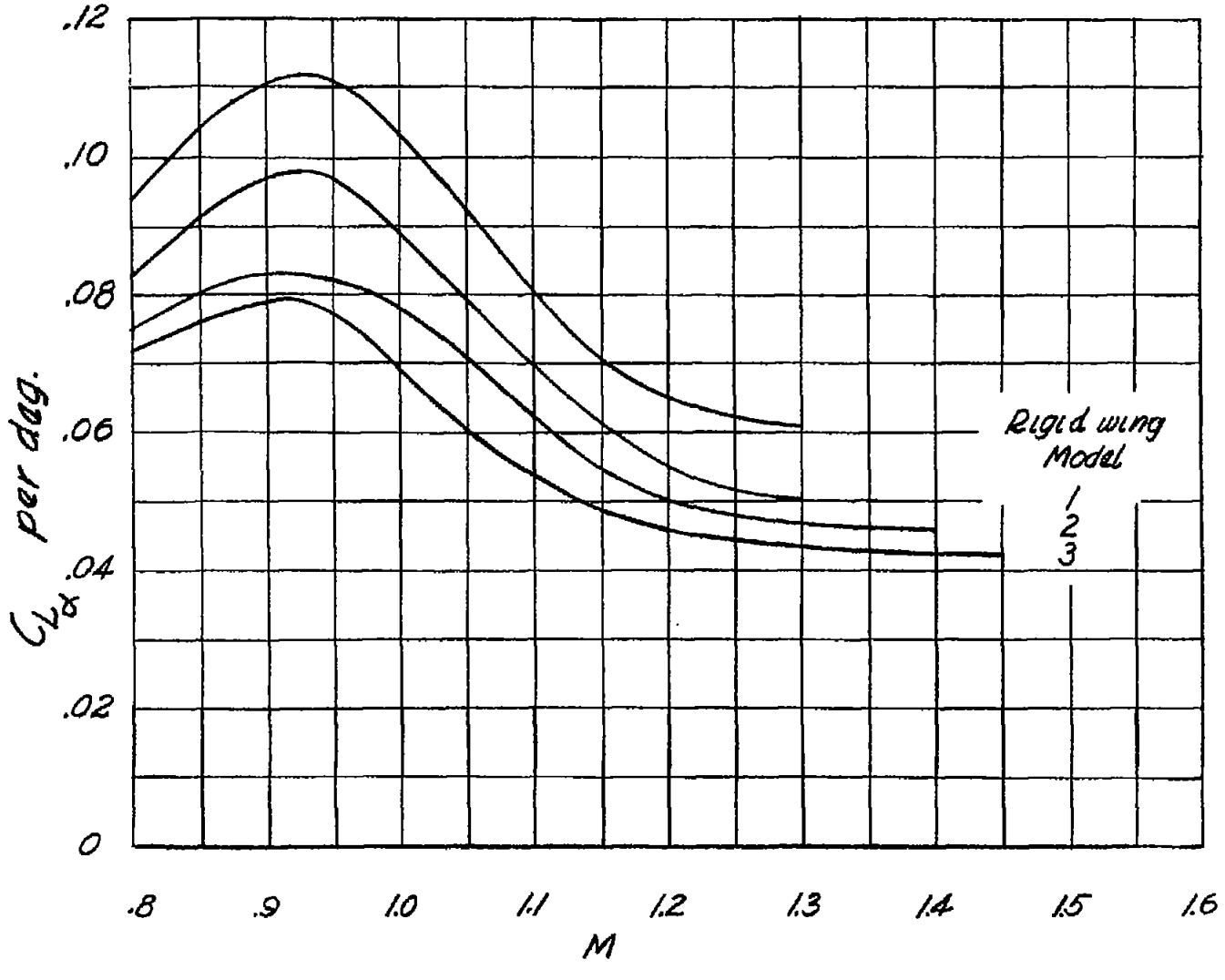

Figure 8.- Variation of C_{L_α} with Mach number for models tested.

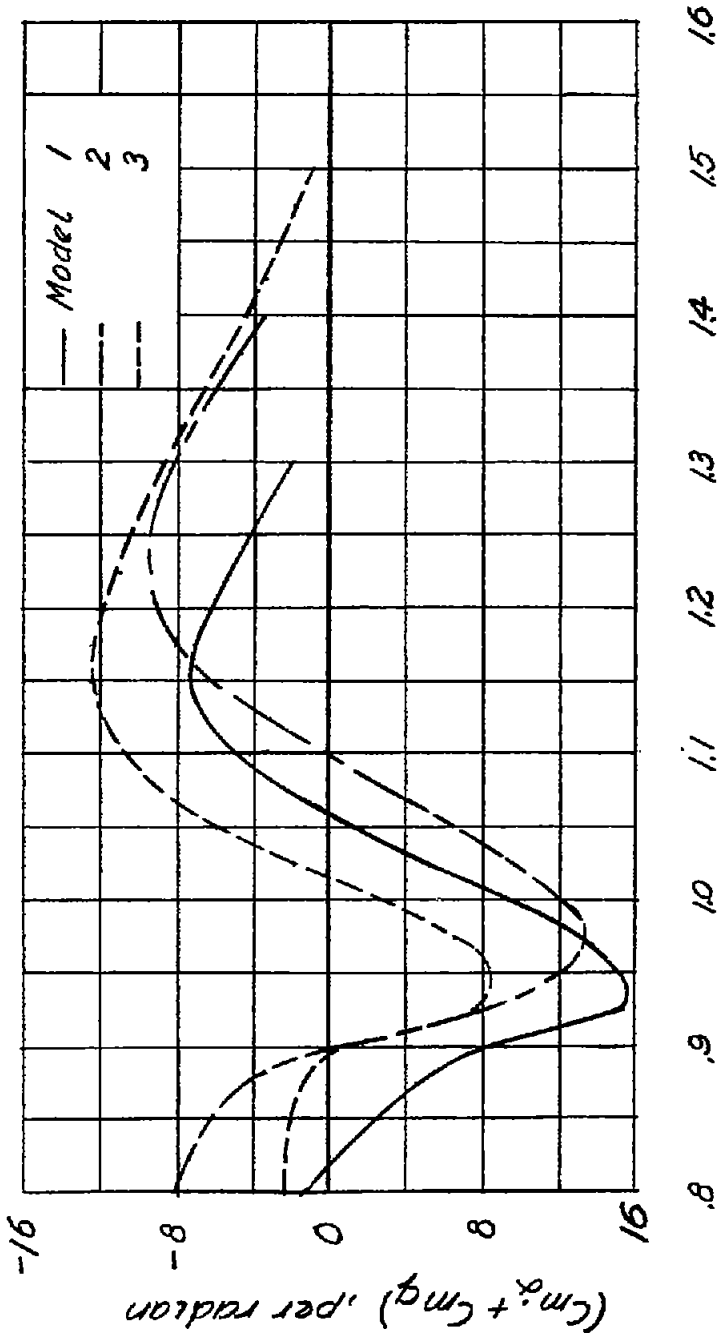

Figure 9.- Variation of damping-moment coefficient with Mach number.

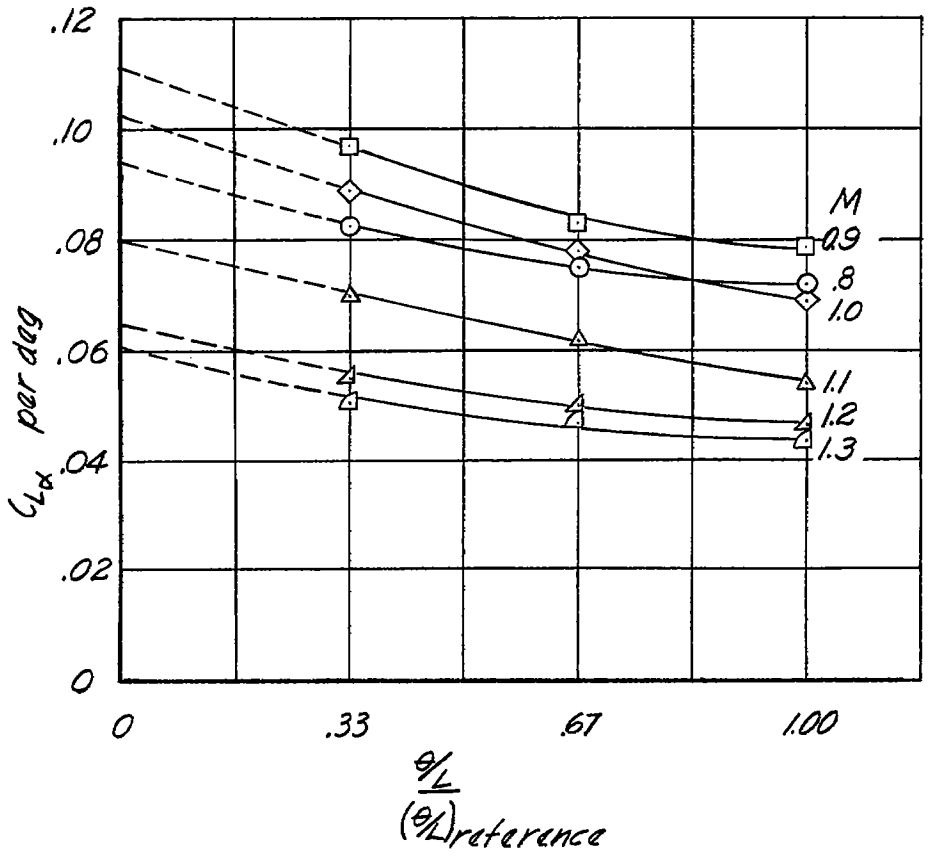

Figure 10.- Extrapolation of experimental lift-curve slopes to rigid-wing values. $\left(\frac{\theta}{L}\right)_{reference}$ = -0.0224 deg/lb.

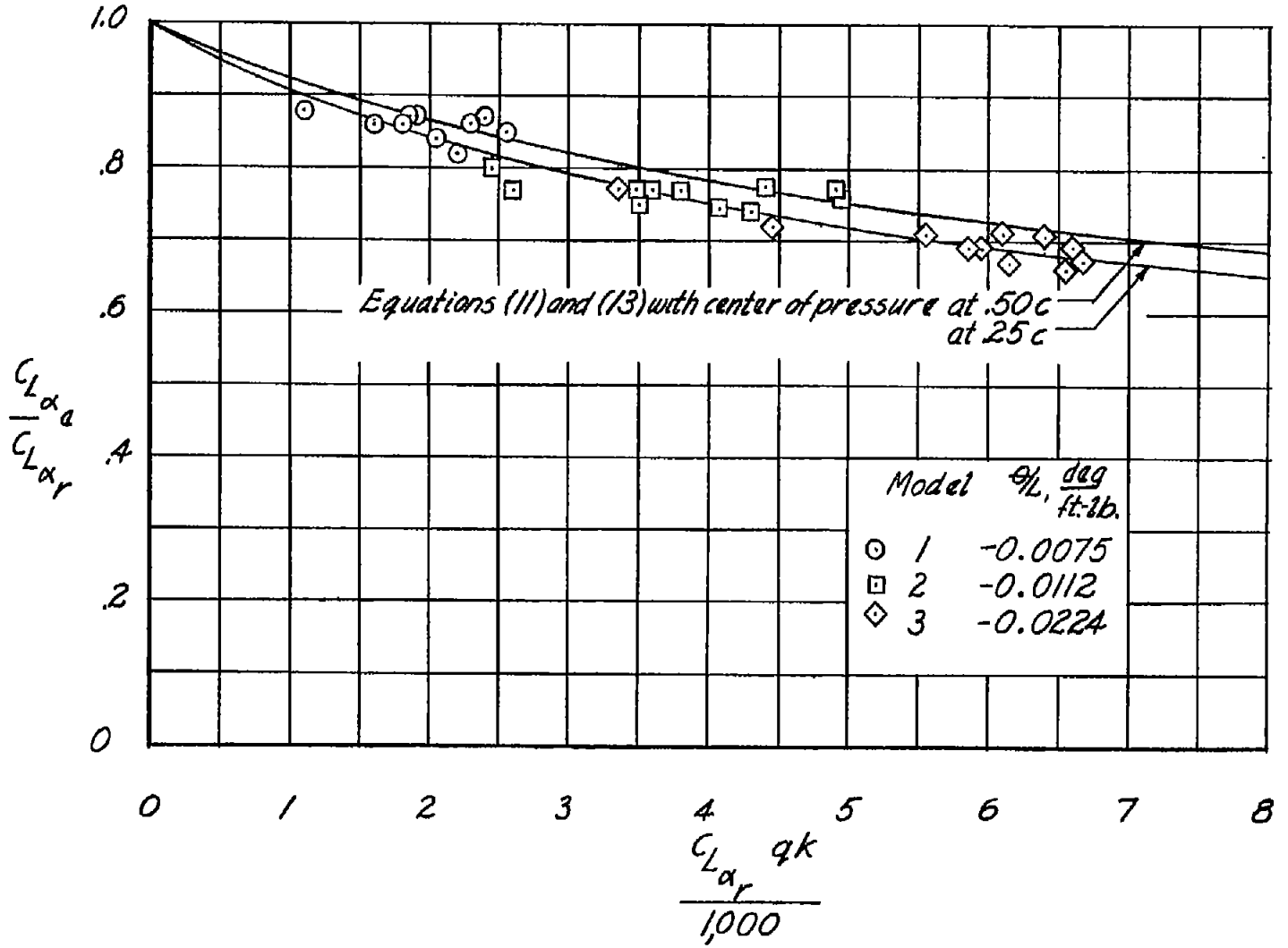

Figure 11.- Comparison of experimental results of effective lift-slope ratio with those predicted by equations (11) and (13).